Fitting Foam Simulation Model Parameters to Data

C. S. Boeije and W. R. Rossen
Department of Geoscience and Engineering
Delft University of Technology

Cheng et al. (2000) present a simple method to fit foam simulation parameters without oil to data for pressure gradient as a function of superficial velocities of gas and liquid. The key in this process is the identification of "high-quality" (high gas fraction) and "low-quality" foam regimes. The method is essentially the same for the foam model parameters in foam models in STARS, UTCHEM or ECLIPSE. Often, however, available data are more limited - pressure gradient for one scan of foam quality at fixed total superficial velocity. We show how to extend this method to the more limited data set. The transition in regimes occurs at the foam quality with the maximum pressure gradient. We illustrate the method by fitting parameters to several published data sets.

Our approach is simple and direct. The model fit would be appropriate for an EOR process involving foam injection at finite water fraction, but not a SAG foam process involving large slugs of gas and liquid. For the latter process, model parameters should be fit to data relevant to that process, i.e. at extremely high foam quality.

The approach assumes an abrupt transition between high- and low-quality foam regimes, i.e. a large value of *epdry* in the STARS foam model. If a smaller value is chosen for faster execution of the simulator this approach could underestimate pressure gradient near its maximum value at the transition between regimes. In that case the parameter values quickly obtained by this method could provide the initial guess for a computer-based least-squares fit of all parameters, including a smaller value of *epdry*, and a check on the parameters so obtained.

Introduction

Gas-injection enhanced-oil-recovery (EOR) processes are efficient at displacing oil where the gas sweeps, but sweep efficiency is poor because of reservoir heterogeneity, viscous instability between injected gas and displaced oil and water, and gravity override of gas. Foam can address all three causes of poor sweep efficiency (Schramm, 1994; Rossen, 1996). Foam is injected in one of three ways: co-injection of gas and surfactant solution, where foam is formed either in the tubing string or immediately as gas and surfactant solution enter the formation; injection of alternating slugs of gas and surfactant solution (SAG), where foam forms in the formation where gas and water meet; and injection of gas alone with surfactant dissolved in the gas, where foam forms in the formation where the injected gas and surfactant meet resident water.

Design of effective foam projects requires accurate simulation of foam behavior in the formation. Cheng et al. (2000) show how to fit the parameters for the STARS and UTCHEM foam simulators describing foam behavior without oil to laboratory coreflood data, specifically a plot of pressure gradient as a function of superficial velocities of gas and water on which contours of pressure gradient are plotted. An example is ***Figure 1***. In such a plot, the "high-quality" foam regime is that at relatively large superficial velocity of gas and small superficial velocity of water, in which the ∇p contours are nearly vertical. (Foam *quality* means gas fractional flow.) The low-quality regime is that at lower superficial velocity of gas and larger velocity of water, in which ∇p contours are nearly horizontal. Cheng et al. suggest that one pick one representative ∇p contour, draw the best horizontal line through the low-quality-regime data and best vertical line through the high-quality-regime data for the same value of ∇p, and fit the foam parameters to the intersection point of these lines. One can then use several horizontal contours in the low-quality regime to fit the shear-thinning behavior in that regime. The fit of Cheng et al. to the data in Figure 1 are shown in ***Figure 2***. This approach assumes that the transition between regimes is abrupt; Cheng et al. argue that the nearly vertical slope seen in data in the high-quality regime suggest an abrupt transition.

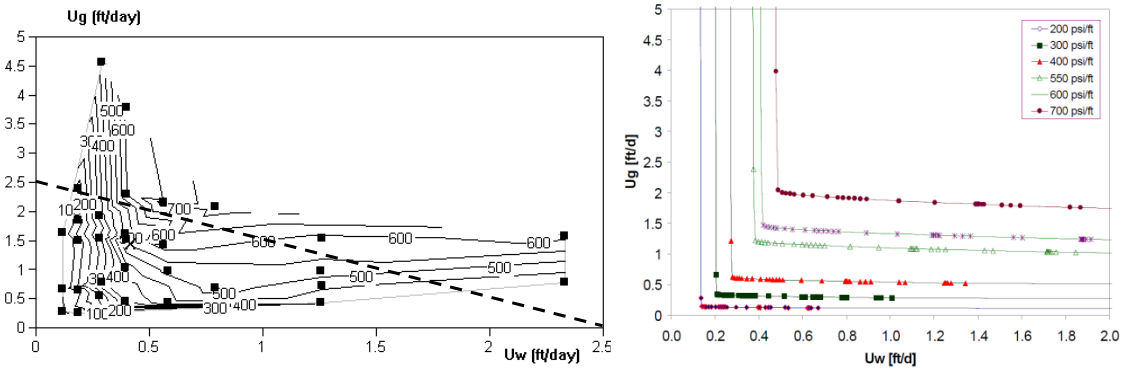

Figure 1 *(left) Pressure gradient (psi/ft) as a function of superficial velocities of gas (Ug) and water (Uw) for one foam formulation in a Berea sandstone core, from Alvarez et al. (2001). Each dot represents a steady-state measurement of pressure gradient, and contours are plotted through these data. The "high-quality" regime is toward the upper left, and the "low-quality" regime to the lower right. The dotted line represents a scan of foam quality at fixed total superficial velocity (in this case, 2.5 ft/day).*
Figure 2 *(right). Fit of Cheng et al. (2000) to these data using the STARS foam model. Symbols are calculated points, not data.*

Ma et al. (2012) present a method for fitting foam parameters to a more-limited set of data, specifically a plot of foam apparent viscosity as a function of foam quality at fixed total superficial velocity. On Figure 1, this data set amounts to a scan along a line joining the same values of superficial velocity on the two axes. In this paper we present a method for fitting parameters to the same sort of data, based on the approach of Cheng et al. (2000). Our approach offers several advantages described below.

The effect of oil on foam is crucial to foam success in the field, but fitting foam parameters in the absence of oil is a necessary first step toward adjusting the model for the effect of oil. Farajzadeh et al. (2012) discuss the challenges of fitting foam models for the effect of oil.

Foam Behavior

Foam is not a new phase but a phenomenon affecting gas and water flow in the presence of surfactant. Foam greatly reduces gas mobility but has little or no direct effect on water mobility. The effect of foam on gas mobility is profound, however.

As noted in the Introduction, in the absence of oil, steady-state foam behavior typically divides into two regimes, illustrated in Figure 1 (Osterloh and Jante, 1992; Alvarez et al., 2001). In the "high-quality" regime, contours of ∇p are nearly vertical, that is, nearly independent of gas superficial velocity. The reason for the nearly vertical contours is the abrupt collapse of foam at a single value of capillary pressure, and therefore a single water saturation, S_w^*, over a range of superficial velocities. If $S_w = S_w^*$ is constant in this regime, then so is water relative permeability; therefore ∇p depends on water superficial velocity but not on gas superficial velocity. In the "low-quality" regime, ∇p is nearly independent of water superficial velocity. The apparent decoupling of ∇p from water flux in this regime could reflect gas trapping and liberation as a function of ∇p (Rossen and Wang, 1999), with no effect on water transport. Behavior in the high-quality regime can be modestly shear-thinning or shear-thickening, but in the low-quality regime it is markedly shear-thinning, reflecting the reduction in gas trapping with increasing ∇p (Rossen and Wang, 1999) as well as the shear-thinning rheology of trains of bubbles (Hirasaki and Lawson, 1985; Xu and Rossen, 2003). The transition between the high-quality and low-quality regimes occurs at a gas fractional flow or foam quality f_g^*; if the transition is abrupt, ∇p is a maximum at f_g^*. Because the low-quality regime is non-Newtonian, the transition foam quality f_g^* is not a constant, however, but varies with total superficial velocity.

Models

Foam models come in two groups. "Population balance models" (Falls et al., 1988; Friedman et al., 1991; Kovscek and Radke, 1994; Kam et al., 2007) represent the dynamics of bubble creation and destruction along with the effect of bubble size on gas mobility. The second group, local-equilibrium (LE) models, represent the effects of bubble size implicitly through a gas-mobility-reduction factor that depends on water saturation, surfactant concentration, and other factors (Law et al., 1989; Patzek and Myhill, 1989; Kular et al., 1989; Fisher et al., 1990; Islam and Farouq-Ali, 1990; Mohammadi and Coombe, 1992; Cheng et al., 2000). LE models are simpler to use, require fewer parameters and avoid some numerical difficulties encountered with population-balance models (though they are not free of numerical challenges themselves). Fitting the parameters of LE models to data is the focus of this study.

One of the most widely used LE foam models is that in STARS, a foam simulator of the Computer Modeling Group (Cheng et al., 2000; Computer Modeling Group, 2007). In this study, the names of parameters will be those in this foam model. Similar models can be found in other simulators such as that in ECLIPSE or UTCHEM, but terminology and some details may vary, as described in Appendix A.

The foam model in STARS introduces a function *FM*, which controls the reduction in gas mobility, into Darcy's law for the gas phase :

$$u_t f_g = -\frac{k k_{rg}^f}{\mu_g}\nabla p = -\frac{k k_{rg} FM}{\mu_g}\nabla p \qquad (1)$$

where k_{rg}^f is the gas relative permeability in the presence of foam and k_{rg} is the gas relative permeability without foam. The latter is assumed to be a known function of phase saturations. The

function *FM* is in turn a product of various other functions (F_1, F_2,… F_6), each of which is aimed at capturing different physical effects. The complete function *FM* is given by (Cheng et al., 2000; Computer Modeling Group, 2006)

$$FM = \frac{1}{1 + fmmob \cdot F_1 \cdot F_2 \cdot F_3 \cdot F_4 \cdot F_5 \cdot F_6} \tag{2}$$

The parameter *fmmob* is the reference gas mobility-reduction factor for wet foams. This parameter corresponds to the maximum attainable mobility reduction. The functions F_1 to F_6 are constrained to values less than or equal to 1, so that each function can only reduce the gas mobility-reduction factor, i.e. increase gas mobility. In this study only the functions F_2 and F_5 are considered; they represent the effects of water saturation and capillary number, respectively, on the behavior of foam. The other functions model the effect of surfactant concentration (F_1), oil saturation (F_3), gas velocity (F_4) and the critical capillary number (F_6); they are not taken into account in this study. The functions F_2 and F_5 are given by

$$F_2 = 0.5 + \frac{\arctan\big(epdry \cdot (S_w - fmdry)\big)}{\pi} \tag{3}$$

$$If\ N_{ca} > fmcap, \qquad F_5 = \left(\frac{fmcap}{N_{ca}}\right)^{epcap}; \qquad else, \qquad F_5 = 1 \tag{4}$$

with

$$N_{ca} \equiv k\nabla p/\sigma_{wg} \tag{5}$$

where σ_{wg} is gas-water surface tension. Factor F_5 makes the low-quality regime non-Newtonian (Cheng et al., 2000). UTCHEM accomplishes this through a similar factor based on gas superficial velocity; see Appendix A.

In total (accounting for these two factors) the foam model contains five parameters (*fmmob*, *epdry*, *fmdry*, *fmcap* and *epcap*).

- If the transition between regimes is abrupt, the parameter *fmdry* is equal to S_w^*, the water saturation at which foam collapses.
- *epdry* controls the abruptness of the foam collapse. Small values give a gradual transition between the two regimes, while larger values yield a sharper, albeit still continuous transition. Reservoir simulators do not work efficiently with discontinuities in fluid properties, and this parameter is commonly tuned so that it does not slow the simulator excessively. This can mean that the modeling of the transition between regimes is not abrupt enough to capture foam behavior seen in the laboratory.
- *epcap* captures the shear-thinning behavior in the low quality regime.
- *fmcap* is a parameter that is set to the smallest capillary number expected to be encountered by foam in the simulation. It is thus not a foam parameter *per se*, though it does affect the values of other parameters.

Fitting Parameters to a Single Scan of Foam Quality

The method of Cheng et al. (2000) requires a substantial amount of data at various gas and water superficial velocities (as in Figure 1) in order to fit model parameters. In some cases, more limited data are available: specifically, a single scan of pressure gradient as a function of foam quality at fixed total superficial velocity. In this section we extend the method of Cheng et al. to this more-limited type of data set, illustrating with various data sets found in literature. One such data set is shown in ***Figure 3***, which is from Ma et al. (2012). Ma et al. plot their results in terms of apparent viscosity instead of pressure gradient; the two sets of data are equivalent, as shown in Eq. 13 below. Ma et al. describe a method of fitting model parameters to the datum with the maximum measured pressure gradient, assuming a relatively gradual transition between the two regimes. Their data are from a

sandpack foam flooding experiment which was conducted with the outlet open to the atmosphere. Thus gas compression may have affected superficial velocity and foam quality in the experiment; for the purpose of illustrating our method of fitting the data we ignore this possibility. The nominal total superficial velocity was kept constant throughout these experiments at 20 ft/day ($7.1 \cdot 10^{-5}$ m/s), but the injected gas fraction varied. Figure 3 clearly shows the two flow regimes (low- and high-quality; compare Figure 3 to ∇p along the dotted line in Figure 1). For low injected gas fractions, the pressure gradient increases with increasing gas fraction. It attains a maximum at a certain gas fraction and, for large gas fractions, the pressure gradient decreases as the gas fraction increases further.

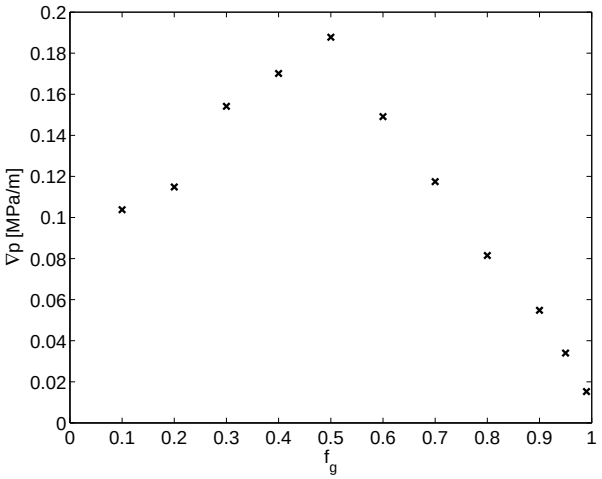

Figure 3 *Scan of foam data at fixed total superficial velocity, after Ma et al. (2012)*

Briefly, the method we propose is as follows. One must know the foam-free relative-permeability functions $k_{rw}(S_w)$ and $k_{rg}(S_w)$ in advance.

1. Plot the best fit through the data in a plot of ∇p v. f_g, as follows:
   - for large values of f_g (the high-quality regime), plot a straight line passing through $(f_g,\nabla p) = (1,0)$
   - for smaller value of f_g (the low-quality regime), plot a convex curve through the data and passing through $(f_g,\nabla p) = (0,0)$
   - f_g^* is the intersection of the line and the curve.
2. Determine *fmdry* from the slope of the straight line through the high-quality-regime data, using Darcy's law for the aqueous phase.
3. Determine *fmmob* from Darcy's law for the gas phase using the value of ∇p at f_g^*.
4. Select a point on the curve through the low-quality-regime data some distance from f_g^*. Fit *epcap* to this datum as described below. Select *fmcap* and adjust *fmmob* according to the range of capillary numbers expected in the simulation, as described below.
5. Pick the largest value of *epdry* consistent with acceptable simulator performance.
6. Plot the resulting fits to the low-quality and high-quality-regime data to verify the fit.

We illustrate the approach using the data of Ma et al. (2012). Appendix B and Table 3 below provide fluid and transport properties used in this model fit in addition to the ∇p data. The first step in fitting the model parameters is determining the foam quality at the transition between the two regimes (f_g^*). Behavior is Newtonian in the high-quality regime (according to the model), and therefore data should fit a straight line through $(f_g,\nabla p) = (1,0)$. The first step then is to plot the best possible straight line through the data in the high-quality regime (f_g greater than that at the maximum in ∇p). If the data cannot be fit well with a straight line through (1,0), it is an indication of either non-Newtonian behavior in the high-quality regime or a less-abrupt collapse of foam at S_w^*; see discussion below.

In the low-quality regime strongly shear thinning behavior is expected, a straight line thought (0,0) would not be expected to fit the data in this regime. Instead we propose that one initially plot a free-

hand convex curve to fit the data in this regime ($f_g < f_g^*$) which also passes through the origin ($\nabla p = 0$ for $f_g = 0$). The intersection between the straight line in the high quality regime and the convex curve in the low quality regime is the estimate for f_g^*. ***Figure 4*** illustrates this method using the data of Ma et al. (2012), where the estimated value of f_g^* is 0.54.

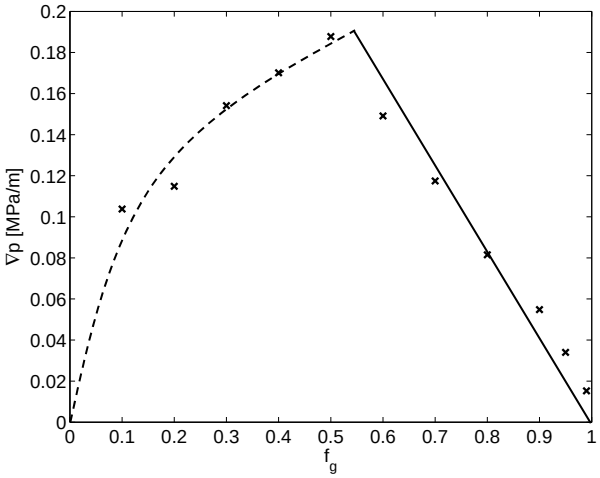

Figure 4 *Data of Ma et al. (2012). Data points are shown as crosses. Initial, hand-drawn, fits to data in low- and high-quality regimes are shown as a convex, dashed curve and a solid straight line respectively.*

The second step is to determine S_w^* from the straight-line fit to the line through the high-quality regime data; throughout this regime $S_w = S_w^*$. Darcy's law applied to the water phase at f_g^* gives

$$u_t(1 - f_g^*) = \frac{k k_{rw}(S_w^*)}{\mu_w} \nabla p(f_g^*) \tag{6}$$

from which (using the known function $k_{rw}(S_w)$) one can determine S_w^*. From the straight line through the data of Ma et al. (2012) we obtain $S_w^* = 0.130$.

The third step is to determine the value of *fmmob* from the pressure gradient at f_g^* using Darcy's law for the gas phase. Because the transition between regimes is abrupt, at f_g^*, $S_w = S_w^*$ *and*

$$FM(f_g^*) = \frac{1}{1 + fmmob} \tag{7}$$

The value of *fmmob* can be obtained from Darcy's law for the gas phase (Eq. (1)) at f_g^*:

$$FM(f_g^*) = \frac{1}{1 + fmmob} = \frac{u_t f_g^* \mu_g}{k k_{rg}(S_w^*)\, \nabla p(f_g^*)} \tag{8}$$

Using the value of S_w^* in Eq. (8) gives $FM(f_g^*) = 3.14 \cdot 10^{-5}$ and thus *fmmob* = $3.18 \cdot 10^4$.

As mentioned, the value of *epdry* is commonly chosen such that the simulator can execute efficiently. In this study we assume that the transition between regimes is abrupt, which corresponds to a large value of *epdry*. We chose *epdry* = 100,000 in most of the fits presented here. The resulting fit to the data of Ma et al. (2012), prior to consideration of shear-thinning in the low-quality regime, is given in ***Figure 5***.

The fit accurately captures the maximum pressure gradient and shows good agreement with the data in the high-quality regime. In the low-quality regime, the fit is less accurate. The model approximates a straight line whereas the data show distinct deviation from a straight line through the origin. This suggests shear-thinning behavior in the low-quality regime, as reported previously (Alvarez et al., 2001).

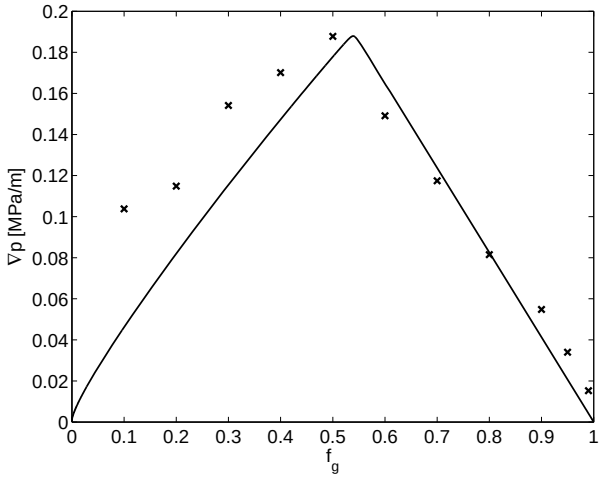

Figure 5 *Model fit to data of Ma et al. (2012) using only the water-saturation-dependent function (F_2). Data points are shown as crosses. The solid line shows the model fit.*

Therefore, the fourth step extends the model using the capillary-number-dependent function (F_5) (Eq. (4)). To simplify the determination of the parameter *epcap* a number of assumptions is made. First, we continue to assume that the transition between regimes is abrupt, i.e. we assume a very large value of *epdry*. This means that the function $F_2 = 1$ throughout the low-quality regime, and can be neglected when fitting the model parameters in this regime. Second, we further assume for simplicity that foam-free gas relative permeability is nearly constant throughout the low-quality regime and is equal to its value at S_w^*. In the final fit obtained below foam-free gas relative permeability changes by only around 10% for the saturations represented by the low-quality data, so initially fixing its value does not cause great errors in the model parameters. We pick one point in the curve through the low-quality data not too close to f_g^*, at a value of f_g we call f_g^+. Our choice is shown in ***Figure 6***. With these assumptions, Darcy's law for the gas phase, applied to this datum, gives:

$$u_t f_g^+ = \frac{k k_{rg}(S_w^*)\,\nabla p(f_g^+)}{\mu_g} \frac{1}{1 + fmmob\left(\dfrac{\nabla p(f_g^*)}{\nabla p(f_g^+)}\right)^{epcap}} \tag{9}$$

Note that for the data to be fit, k and σ_{wg} are fixed, so the ratio of capillary numbers in Eq. 4 equals the ratio of pressure gradients. This equation can be rearranged into an expression for *epcap*:

$$epcap = \frac{\log\left(\dfrac{k k_{rg}(S_w^*)\,\nabla p - u_t\, f_g^+ \mu_g}{fmmob\;\mu_g\, f_g}\right)}{\log\left(\dfrac{\nabla p(f_g^*)}{\nabla p(f_g^+)}\right)} \tag{10}$$

This approach yields the value of *epcap*. Since F_5 is constrained to values less than 1, the value of *fmcap* cannot be set by ∇p at f_g^*, the experimentally observed maximum value of ∇p; F_5 would then simply return a value of 1 (Eq. 4) for smaller values of pressure gradient, including those in the low-quality regime used to fit the parameters. Instead, *fmcap* should be based on either the lowest value of ∇p expected in the simulation, or a lower limit below which non-Newtonian effects are not expected; call this value ∇p_{lim}. In addition, the value of *fmmob* must be adjusted; let $fmmob^*$ be the value derived above at f_g^*; the new value of *fmmob* is given by

$$fmmob = fmmob^* \left(\frac{\nabla p(f_g^*)}{\nabla p_{lim}}\right)^{epcap} \tag{11}$$

For illustration, here we choose $\nabla p_{lim} = \nabla p(f_g^*)/5$. Allowing for shear-thinning in the low-quality regime increases the value of *fmmob*, which can be problematic for simulators at low superficial velocity. The resulting fit for ∇p in the low-quality regime is given by the following expression, which is an approximation for the case *fmmob* >> 1, and illustrated in Figure 6:

$$\nabla p = \left(\frac{f_g \, u_t \, \mu_g \, fmmob \, \nabla p_{lim}^{epcap}}{k \, k_{rg}(S_w^*)} \right)^{\frac{1}{1+epcap}} \qquad (12)$$

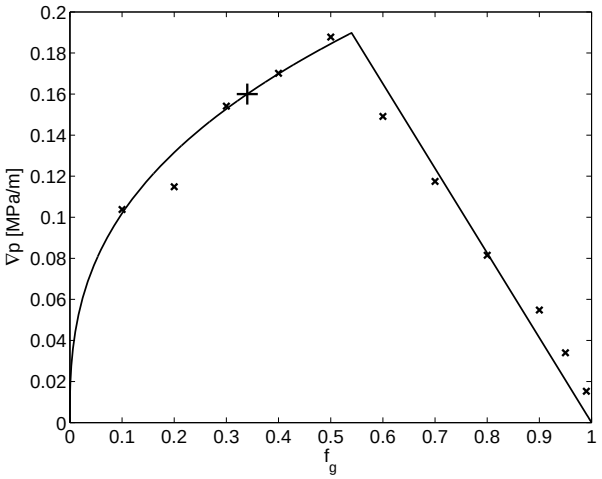

Figure 6 *Model fit to data of Ma et al. (2012) including the capillary-number-dependent function (F_5) in the low-quality regime. Data points in the low- and high-quality regimes are shown by crosses. The solid line shows the model fit. The '+' sign is the chosen value of* (f_g^+, $\nabla p(f_g^+)$).

Other Examples

We illustrate the fit of model parameters using data from various other published studies. The data of Alvarez et al. (2001) and fit of Cheng et al. (2000) are shown in Figures 1 and 2. Here we take a scan of ∇p at fixed a superficial velocity of 2.5 ft/day ($8.8 \cdot 10^{-6}$ m/s). The data in this case are values read off ∇p contours on the diagonal line on Figure 1. These experiments were carried out using Berea sandstone rather than the sandpacks that were used in the experiments of Ma et al. Therefore, different relative-permeability functions were used, as described in Appendix B. ***Figures 7*** and **8** show the model fit with and without including the effects of shear-thinning in the low-quality regime. In this case we use a value of *epdry* of 20,000 for direct comparison with fit by Cheng et al. (2000) and also use the same value of *fmcap* as in that study.

Table 1 compares the results obtained here to those of Cheng et al. (2000). The value of the parameter *fmcap* is calculated using a surface tension σ_{wg} = 0.03 N/m, a typical value for surfactant solutions against N_2 gas at room temperature and atmospheric pressure (Rossen, 1996). The fit of Cheng et al. to the data in Fig. 1 give similar values of *epcap* and *fmdry* to those we obtain from a scan of foam quality at a single total superficial velocity. In the course of making our fit we discovered an error in the calculations of Cheng et al., probably arising from a units conversion from (1/ft) to (1/m); that is, the values of ∇p from their model in the low-quality regime are factor 3.28 lower than the ∇p data. The value of *fmmob* is therefore too small by a factor $(3.28)^{(1+epcap)}$. When corrected for this error (Table 1) our value of *fmmob* is close to theirs.

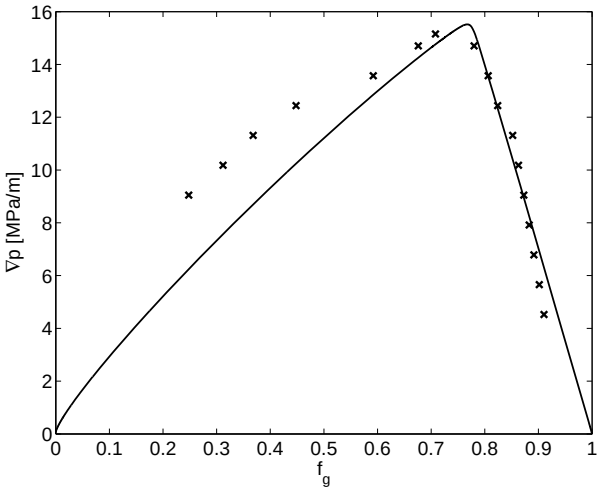

Figure 7 *Model fit to the data of Alvarez et al. (2001) using only the water-saturation-dependent function F_2. Parameter values are* fmmob = $4.27 \cdot 10^4$, fmdry = 0.311, $f_g^* = 0.775$

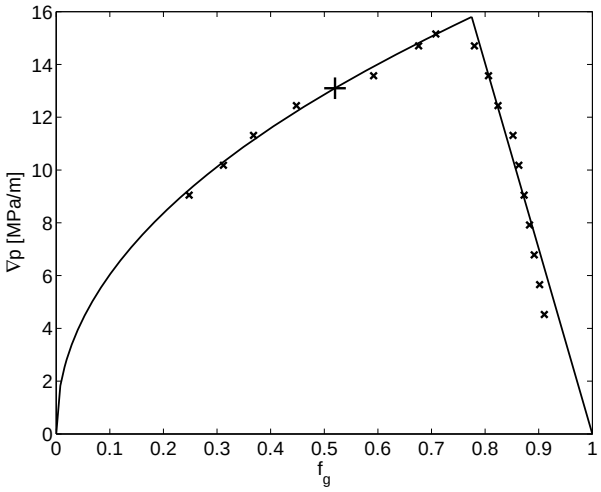

Figure 8 *Model fit to the data of Alvarez et al. (2001) including the capillary-number-dependent function F_5. Parameter values are* fmmob = $6.63 \cdot 10^5$, fmdry = 0.311, epcap = 1.13, fmcap = $2.46 \cdot 10^{-5}$. *The '+' sign is the chosen value of* (f_g^+, $\nabla p(f_g^+)$).

Table 1 *Comparison of results from this study with Cheng et al. (2000)*

	Cheng et al. (2000)	**This study**
fmmob	$6.84 \cdot 10^{5\dagger}$	$6.63 \cdot 10^5$
*fmmob**		$4.27 \cdot 10^4$
epdry	$2.00 \cdot 10^4$	$2.00 \cdot 10^4$
fmdry	0.316	0.311
fmcap	$2.46 \cdot 10^{-5}$	$2.46 \cdot 10^{-5}$
epcap	1.12	1.13

† adjusted from that given in Cheng et al. (2000) as described in text

Moradi-Araghi et al. (1997) quantify foaming performance with plots of gas fraction (f_g) vs. mobility reduction factor *RF*, defined as the ratio of the pressure drop during foam injection to that during brine injection ($RF \equiv \Delta p_{foam}/\Delta p_{brine}$). To convert *RF* to a pressure gradient, the total superficial velocity u_t is required. However, this is not provided in the paper. Instead we plot these data as gas fraction vs. apparent viscosity of foam μ_{app}. The latter is defined by

$$\mu_{app} \equiv \frac{k\nabla p}{u_t} \equiv RF \cdot \mu_w \qquad (13)$$

Thus the mobility-reduction factor RF can easily be converted to apparent viscosity using brine viscosity, but not to ∇p without knowing u_t. Since the ratio $(\nabla p/u_t) = (RF\ \mu_w/k)$ occurs in Eqs. 6, 8, 9 and 10 it is possible to solve for model parameters (except *fmcap*) without knowing u_t. The experiments of Moradi-Araghi et al. were performed at a temperature of 98°F (36.7°C) at which brine viscosity is approximately 0.69 mPa·s. These experiments were performed in sandstone so we use the same relative-permeability functions as for the model fits to the data by Alvarez et al. (Eqs. B4 and B5). The resulting model fits are shown in ***Figures 9*** and ***10***.

Other data from Moradi-Araghi for foam in a 496-md core are fit in **Figures 11** and **12**.

Another recent data set can be found in Chabert et al. (2012), who conducted CO_2 foam flooding tests in low-permeability (20 mD) Indiana limestone cores. For carbonates we use yet another set of relative permeability functions, as described in Appendix B. The fit to the data of Chabert et al. is

given in ***Figure 13***. In this case foam reduces gas mobility much less than in the other cases (*fmmob* = 5.50), and a satisfactory fit is obtained to low-quality-regime data without adjusting for non-Newtonian behavior there; thus we make no fit for *epcap* or *fmcap*. In this case the pressure gradient in the absence of foam ($f_g \rightarrow 0$ or 1) is of the same order of magnitude as that with foam. The kink in the predicted curve for $\nabla p(f_g)$ for f_g close to 1 represents $S_w <$ *fmdry* - foam drier than the high-quality regime. (Such behaviour is suggested by Alvarez et al. at very large f_g in their case). The trend predicted for the high-quality regime remains a straight line through $(f_g, \nabla p) = (1,0)$.

An overview of the input parameters used is given in ***Table 2*** and all of the derived foam parameter values are given in ***Table 3***.

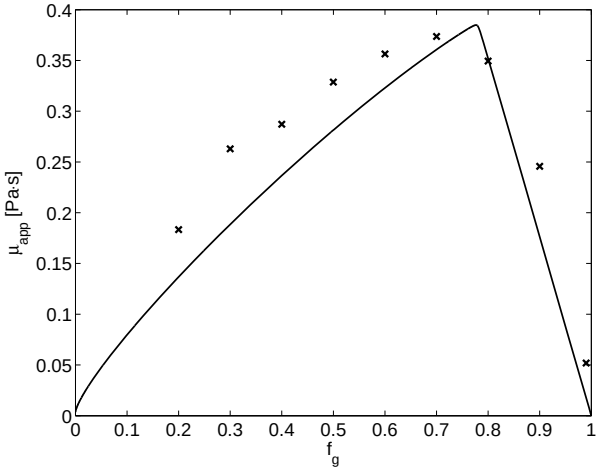

Figure 9 *Model fit to the data of Moradi-Araghi et al. (1997) using only the water-saturation-dependent function F_2. Parameter values are* fmmob = $5.57 \cdot 10^3$, fmdry = 0.336, $f_g^* = 0.78$

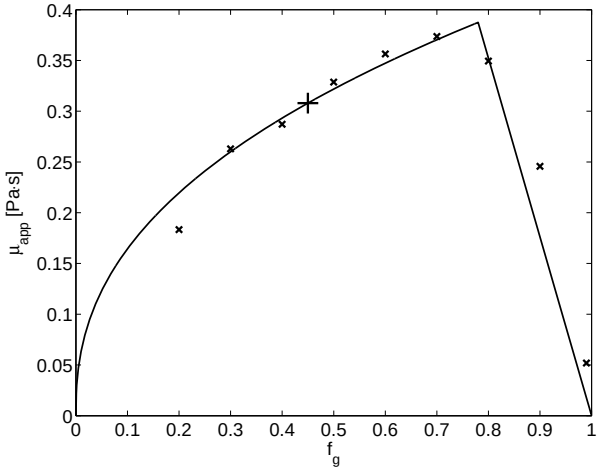

Figure 10 *Model fit to the data of Moradi-Araghi et al. (1997) including the capillary-number-dependent function F_5. Parameter values are* fmmob = $5.26 \cdot 10^4$, epcap = 1.40. *The '+' sign is the chosen value of* $(f_g^+, \mu_{app}(f_g^+))$

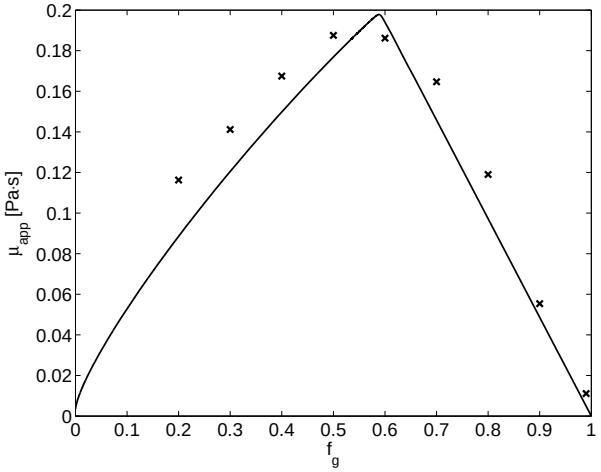

Figure 11 *Model fit to the data of Moradi-Araghi et al. (1997) using only the water-saturation-dependent function F_2. Parameter values are* fmmob = $3.28 \cdot 10^3$, fmdry = 0.385, $f_g^* = 0.59$

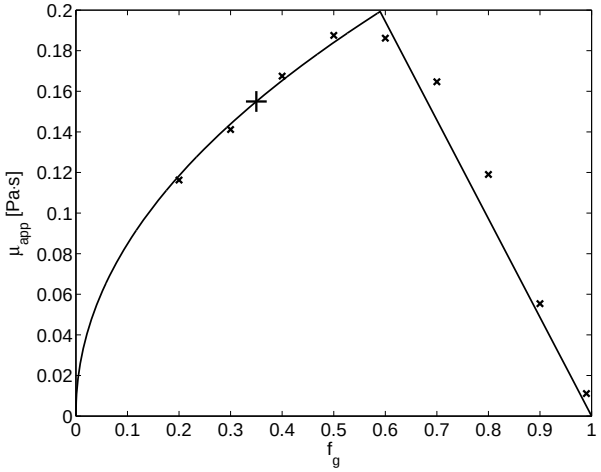

Figure 12 *Model fit to the data of Moradi-Araghi et al. (1997) including the capillary-number-dependent function F_5. Parameter values are* fmmob = $1.86 \cdot 10^4$, epcap = 1.08. *The '+' sign is the chosen value of* $(f_g^+, \mu_{app}(f_g^+))$

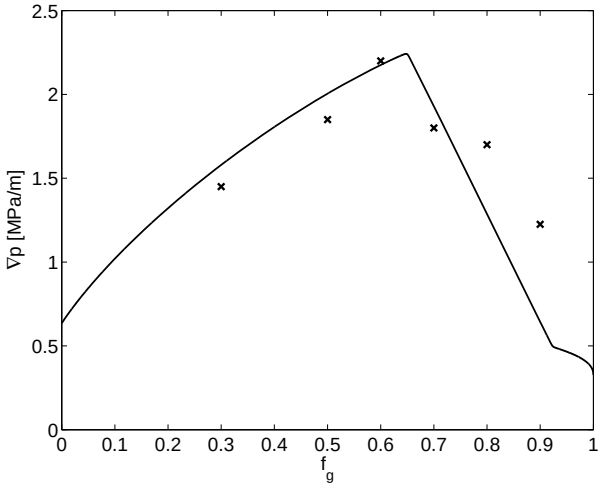

Figure 13 *Model fit to the data of Chabert et al. (2012) using only the water-saturation-dependent function F_2. Parameter values are* fmmob = 5.5, fmdry = 0.550, $f_g^* = 0.65$.

Table 2 *Overview of input parameters for all of the investigated studies*

	Ma et al. (2012)	**Alvarez et al. (2001)**	**Moradi-Araghi et al. (1) (1997)**	**Moradi-Araghi et al. (2) (1997)**	**Chabert et al. (2012)**
Porous medium	Unconsolidated sand	Sandstone	Sandstone	Sandstone	Limestone
μ_w (Pa·s)	$1.0 \cdot 10^{-3}$	$0.70 \cdot 10^{-3}$	$0.69 \cdot 10^{-3}$	$0.69 \cdot 10^{-3}$	$0.65 \cdot 10^{-3}$
μ_g (Pa·s)	$2.0 \cdot 10^{-5}$	$2.0 \cdot 10^{-5}$	$6.0 \cdot 10^{-5}$	$6.0 \cdot 10^{-5}$	$6.0 \cdot 10^{-5}$
Type of gas	Air	N_2	CO_2	CO_2	CO_2
σ_{wg} (N/m)	0.030	0.030	0.005	0.005	0.005
u_t (m/s)	$7.1 \cdot 10^{-5}$	$8.8 \cdot 10^{-6}$	Unknown	Unknown	$5.4 \cdot 10^{-6}$
T (°C)	20	20	37	37	40
k (m^2)	$1.58 \cdot 10^{-10}$	$5.30 \cdot 10^{-13}$	$5.52 \cdot 10^{-13}$	$4.96 \cdot 10^{-13}$	$2.0 \cdot 10^{-14}$
Backpressure (Pa)	0	$4.14 \cdot 10^{6}$	$1.38 \cdot 10^{7}$	$1.38 \cdot 10^{7}$	$1.30 \cdot 10^{7}$

Table 3 *Fitted values of STARS foam model parameters*

	Ma et al. (2012)	**Alvarez et al. (2001)**	**Moradi-Araghi et al. (1) (1997)**	**Moradi-Araghi et al. (2) (1997)**	**Chabert et al. (2012)**
fmmob	$4.99 \cdot 10^{5}$	$6.63 \cdot 10^{5}$	$5.26 \cdot 10^{4}$	$1.86 \cdot 10^{4}$	5.5
*fmmob**	$3.18 \cdot 10^{4}$	$4.27 \cdot 10^{4}$	$5.57 \cdot 10^{3}$	$3.28 \cdot 10^{3}$	-
epdry	$1.00 \cdot 10^{5}$	$2.00 \cdot 10^{4}$	$1.00 \cdot 10^{5}$	$1.00 \cdot 10^{5}$	$1.00 \cdot 10^{5}$
fmdry	0.130	0.311	0.336	0.385	0.550
fmcap	$2.00 \cdot 10^{-4}$	$2.46 \cdot 10^{-5}$	Unknown†	Unknown†	-
epcap	1.71	1.13	1.40	1.08	-
f_g^*	0.54	0.775	0.78	0.59	0.65

† - N_{ca} and *fmcap* are unknown because u_t is unspecified. We can still fit non-Newtonian behavior using ratios of *RF*, which at fixed superficial velocity equal the ratios of N_{ca}.

Discussion

The model-fitting approach presented here has the following advantages:

1. The approach is simple. It can be carried out directly from a plot of the raw data using a pencil and a calculator.

2. It begins by making the best fit to both regimes based on all data in that regime. It allows that the transition in regimes, and the maximum in ∇p, may occur between measured values of f_g.
3. The approach directly incorporates the assumptions of the STARS foam model into the process from the first step. Excessive scatter or a mismatch between the data and model assumptions is immediately apparent.
4. Direct involvement of the user in the fitting process helps ensure understanding of the model parameters obtained.

The approach does suffer from the following shortcomings:

1. The fit obtained is not necessarily the least-squares fit to the data. The user must judge for himself in the last step (6) whether the fit is adequate.
2. The approach assumes an abrupt transition between high- and low-quality regimes, i.e. a large value of *epdry* in the STARS model. If a relatively small value of *epdry* is selected for the sake of faster simulator execution times, then in particular the model fit may somewhat underestimate ∇p at f_g^*. ***Figure 14*** shows the effect of the value of *epdry* on the fit to data of Ma et al. (cf. Figure 6), holding all other parameters constant. In that case we believe the parameters quickly obtained by this method could provide the initial guess for a computer-based least-squares fit of all parameters, including a smaller value of *epdry*, and a check on the parameters so obtained.

   A curved, convex trend for all the data, as for the model fit with *epdry* = 100 in Figure 14, could indicate that a smaller value of *epdry* would give a better fit to the data than assumed in our approach. Of the five data sets shown here, only that in Figure 9 shows such consistent curved, convex trend through all the data.
3. The method proposed here is appropriate for a process of foam injection with finite injected water fraction. In a SAG (surfactant-alternating-gas) process, behavior during gas injection depends on foam properties at very low water fraction (Zhou and Rossen, 1995; Rossen et al., 1999; Shan and Rossen, 2004); properties at larger water fraction are relatively unimportant to the process, and data should be fit specifically to this low range of water fraction (cf. Kibodeaux and Rossen, 1997; Xu and Rossen, 2004; Rossen and Bruining, 2007).
4. A scan of foam quality at a single superficial velocity is a more limited data set than that used by Cheng et al. (2000). In using such a data set, one risks failing to notice deviations from the assumptions of the foam model. Not all foam data show horizontal ∇p contours in the low-quality regime, for instance (Kim et al., 2005). A scan of foam quality at fixed superficial velocity could fail to detect this deviation.

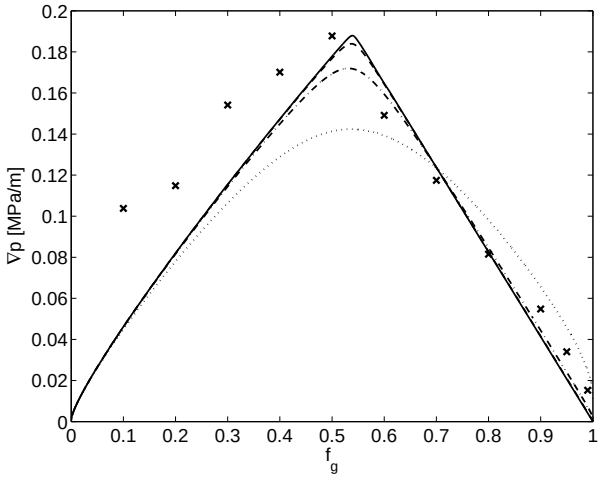

Figure 14 *Effect of* epdry *on model fit to data of Ma et al. (2012) excluding for simplicity the capillary-number-dependent function (*F_5*) in the low-quality regime. Curves correspond to the following values of* epdry*: 100,000, 10,000, 1,000, 100.*

Conclusions

We present a method for fitting parameters in the STARS foam model (excluding the effect of oil) to data for pressure gradient ∇p (or, equivalently, resistance factor RF or apparent viscosity μ_{app}) as a function of foam quality at a single superficial velocity. The approach estimates the non-Newtonian behavior in the low-quality regime from the same set of data. The same method would apply to the parameters of the foam model in ECLIPSE, and a similar method to those in UTCHEM. Its advantages are simplicity and directness. The model fit would be appropriate for an EOR process involving foam injection at finite water fraction, but not a SAG foam process involving large slugs of gas and liquid. For the latter process model parameters should be fit to data relevant to that process, i.e. at extremely high foam quality.

This approach assumes an abrupt transition between high- and low-quality foam regimes, i.e. a large value of *epdry*, and if a relatively small value is chosen for faster execution of the simulator this approach would underestimate ∇p near its maximum. In that case the parameter values quickly obtained by this method could provide the initial guess for a computer-based least-squares fit of all parameters, including a smaller value of *epdry*, and a check on the parameters so obtained.

Acknowledgements

We gratefully acknowledge the financial support of Maersk Oil, and especially helpful discussions with Dr. K. Mogensen. Also, we thank Prof. G.J. Hirasaki of Rice University for helpful discussions and for supplying us with experimental data (those of Ma et al. (2012)) that were used in this study.

References

Alvarez, J. M., Rivas, H., and Rossen, W. R., "A Unified Model for Steady-State Foam Behavior at High and Low Foam Qualities," SPE 74141, *SPE Journal* **6**, 325-333(2001).

Chabert, M., Morvan, M., and Nabzar, L., "Advanced screening technologies for the selection of dense CO_2 foaming surfactants", paper SPE 154147 presented at the Eighteenth SPE Improved Oil Recovery Symposium, Tulsa, OK, 14-18 April 2012.

Cheng, L., Reme, A. B., Shan, D., Coombe, D. A. and Rossen, W. R., "Simulating Foam Processes at High and Low Foam Qualities," paper SPE 59287 presented at the 2000 SPE/DOE Symposium on Improved Oil Recovery, Tulsa, OK, 3-5 April.

Computer Modeling Group, *STARS User's Guide*, Version 2006, Calgary, Alberta, Canada.

Dong, Y., and Rossen, W. R., "Insights from Fractional-Flow Theory for Models for Foam IOR," 14th European Symposium on Improved Oil Recovery, Cairo, Egypt, 22-24 April, 2007.

Falls, A. H., Hirasaki, G. J., Patzek, T. W., Gauglitz, D. A., Miller, D. D., and Ratulowski, J, "Development of a Mechanistic Foam Simulator: The Population Balance and Generation by Snap-Off," *SPE Reser. Eng*. **3**, 884-892 (1988).

Farajzadeh, R., Andrianov, A., Krastev, R., Hirasaki, G. J., and Rossen, W. R., "Foam-Oil Interaction in Porous Media: Implications for Foam Assisted Enhanced Oil Recovery," *Adv. Colloid Interface Sci.*, **183-184**, 1-13 (2012).

Fisher, A. W., Foulser, R. W. S., and Goodyear, S. G., "Mathematical Modeling of Foam Flooding," SPE/DOE 20195 presented at the 1990 SPE/DOE Symposium on Enhanced Oil Recovery, Tulsa, OK, Apr. 22-25.

Friedmann, F., Chen, W. H., and Gauglitz, P. A., "Experimental and Simulation Study of High-Temperature Foam Displacement in Porous Media," *SPE Reser. Eng*. **6**, 37-75 (1991).

Hirasaki, G.J., and Lawson, J.B., "Mechanisms of Foam Flow in Porous Media: Apparent Viscosity in Smooth Capillaries", *SPE Journal* **25**, 176-190 (1985).

Islam, M. R. and Farouq-Ali, S. M., "Numerical Simulation of Foam Flow in Porous Media," *J. Canadian. Pet. Tech*. (July-Aug. 1990) 47-51.

Kam, S. I., Nguyen, Q. P., Li, Q., and Rossen, W. R., "Dynamic Simulations With an Improved Model for Foam Generation," *SPE Journal* **12**, 35-48 (2007).

Kibodeaux, K. R., and Rossen, W. R., "Coreflood Study of Surfactant-Alternating-Gas Foam Processes: Implications for Field Design," paper SPE 38318 presented at the 1997 SPE Western Regional Meeting, Long Beach, CA, June 25-27.

Kim, J. S., Dong., Y., and Rossen, W. R., "Steady-State Flow Behavior of CO_2 Foam," *SPE Journal* **10**, 405-415 (2005).

Kovscek, A. R. and Radke, C. J., "Fundamentals of Foam Transport in Porous Media," in *Foams: Fundamentals and Applications in the Petroleum Industry*, L.L. Schramm (ed.) ACS Advances in Chemistry Series, Am. Chem. Soc., Washington, D.C. (1994) 3, No. 242.

Kular, G. S., Lowe, K., and Coombe, D., "Foam Application in an Oil Sands Steam Flood Process," paper SPE 19690 presented at the 1989 SPE Annual Tech. Conf. and Exhibition, San Antonio, TX, Oct. 8-11.

Law, D. H., Yang, Z.-M., and Stone, T., "Effect of Presence of Oil on Foam Performance: A Field Simulation Study," paper SPE 18721 presented at the 1989 SPE Symposium on Reservoir Simulation, Houston, TX, Feb. 6-8.

Ma, K., Biswal. S. L., and Hirasaki, G. J., "Experimental and Simulation Studies of Foam in Porous Media at Steady State," presented at the 2012 AIChE Spring Meeting, Houston, TX, 1-5 April, 2012.

Mohammadi, S., and Coombe, D. A., "Characteristics of Steam-Foam Drive Process in Massive Multi-Zone and Thin Single-Zone Reservoirs," paper 14030, presented at the 1992 SPE Western Regional Meeting, Bakersfield, CA, March 30-April 1.

Mohamed, I. M., and Nasr-El-Din, H. A., "Formation Damage Due to CO_2 Sequestration in Deep Saline Carbonate Aquifers," paper SPE 151142 presented at the SPE International Symposium and Exhibition on Formation Damage Control, Lafayette, LA, 15-17 February 2012.

Moradi-Araghi, A., Johnston, E. L., Zornes, D. R., and Harpole, K. J., "Laboratory Evaluation of Surfactants for CO_2-Foam Applications at the South Cowden Unit", paper SPE 37218 presented at the 1997 SPE International Symposium on Oilfield Chemistry, Houston, 18-21 February.

Osterloh, W. T., and Jante, M. J., "Effects of Gas and Liquid Velocity on Steady-State Foam Flow at High Temperature," paper SPE/DOE 24179, presented at the 1992 SPE/DOE EOR symposium, Tulsa, OK, April 22-24.

Patzek, T. W. and Myhill, N. A., "Simulation of the Bishop Steam Foam Pilot," paper SPE 18786 presented at the 1989 SPE California Regional Meeting, Bakersfield, Apr. 5-7.

Persoff, P., Pruess, K., Benson, S. M., Wu, Y. S., Radke, C. J., and Witherspoon, P. A., "Aqueous Foams for Control of Gas Migration and Water Coning in Aquifer Gas Storage," *Energy Sources* **12**, 479-497 (1990).

Rossen, W.R., "Foams in Enhanced Oil Recovery," in R. K. Prud'homme and S. Khan, ed., *Foams: Theory, Measurements and Applications*, Marcel Dekker, New York (1996), pp. 413-464.

Rossen, W. R., and Bruining, J., "Foam Displacements With Multiple Steady States," *SPE Journal* **12**, 5-18 (2007).

Rossen, W. R., and Wang, M. W., "Modeling Foams for Acid Diversion", *SPE Journal* **4**, 92-100 (1999).

Rossen, W. R., Zeilinger, S. C., Shi, J.-X., and Lim, M. T., "Simplified Mechanistic Simulation of Foam Processes in Porous Media," *SPE Journal* **4**, 279-287 (1999).

Schlumberger, *ECLIPSE* Reservoir Simulation Software, Version 2010.2, Technical Description*, 2010.

Schramm, L. L. (ed.) *Foams: Fundamentals and Applications in the Petroleum Industry*, ACS Advances in Chemistry Series No. 242, Am. Chem. Soc., Washington, DC (1994).

Shan, D. and Rossen, W. R., "Optimal Injection Strategies for Foam IOR," *SPE Journal* **9**, 132-150 (2004).

Xu, Q., and Rossen, W. R., "Effective Viscosity of Foam in Periodically Constricted Tubes," *Colloids Surfaces A: Physicochem Eng. Aspects* **216**, 175-194 (2003).

Xu, Q., and Rossen, W. R., "Experimental Study of Gas Injection in Surfactant-Alternating-Gas Foam Process," *SPE Reservoir Eval, Eng*. **7**, 438-448 (2004).

Zhou, Z. H. and Rossen, W. R,. "Applying Fractional-Flow Theory to Foam Processes at the 'Limiting Capillary Pressure'," *SPE Adv. Technol*. **3**, 154-162 (1995).

Appendix A. Relation of Foam Parameters in Other Foam Models to Those in STARS

Table A1 lists the STARS foam model parameters used in this study and the corresponding parameters in the foam models in ECLIPSE (Schlumberger, 2010) and UTCHEM (Cheng et al., 2000). The parameter names listed here for ECLIPSE and UTCHEM are not necessarily the variable names in the code, but rather names defined in the simulators' reference manuals (or, for UTCHEM, in Cheng et al. (2000)). Also note that the UTCHEM model has some differences with the STARS model (e.g., shear-thinning rheology is based on gas superficial velocity rather than capillary number).

Table A1: *Foam model parameter terminology in three different reservoir simulators*

STARS	ECLIPSE	UTCHEM
fmmob	M_r	R
epdry	f_w	ε
fmdry	$S_w^{\,l}$	$S_w^{\,*}$
fmcap	$N_c^{\,r}$	u_g
epcap	e_c	σ

Note that in some cases the simulators use symbols with conventional definitions different from those in the reference manual. In particular, in the ECLIPSE foam model f_w is not water fractional flow but a parameter like *epdry*, and in UTCHEM σ is not surface tension but a power-law parameter for shear-thinning foam.

The ECLIPSE foam model is substantially similar to that in STARS in how it handles the two effects that are the focus of this study. UTCHEM differs in some ways. Instead of Eq. 3 UTCHEM interpolates the mobility-reduction factor between R (its value in the low-quality regime) and 1 over an interval ($S_w^{\,*} \pm \varepsilon$). Thus a small value of ε corresponds to a large value of *epdry* in STARS. The differences between these methods of interpolation of mobility reduction as a function of S_w have a major impact on the modeling of SAG foam floods (Dong and Rossen, 2007), but these differences are outside the scope of this study. Also, UTCHEM represents shear-thinning in the low-quality regime as a function of gas superficial velocity rather than capillary number, which simplifies the fitting of the shear-thinning parameter σ from the procedure for *epcap* we outline above. Cheng et al. note that σ, the power-law exponent for foam, is related to *epcap* by

$$\sigma = 1 / (1 + epcap) \tag{A1}$$

Appendix B. Transport Functions and Fluid Properties Used in Model Fits

To represent the experiments of Ma et al. (2012) in a sandpack we start with relative-permeability expressions from Kam and Rossen (2003) which are based on a fit to sandpack relative-permeability data:

$$k_{rg} = \left(\frac{1 - S_w - S_{gr}}{1 - S_{wc} - S_{gr}} \right)^{2.2868} \tag{B1}$$

$$k_{rw} = 0.7888 \left(\frac{S_w - S_{wc}}{1 - S_{wc} - S_{gr}} \right)^{1.9575} \tag{B2}$$

In these expressions, S_{gr} and S_{wc} are respectively the residual gas saturation and the connate water saturation. We assume both are equal to 0.05 in our fit to the data (the value of S_{wc} is similar to that implied in the foam data of Osterloh and Jante (1992)). Ma et al. also measured water saturation in the sandpack during the experiments. Their saturation data suggest a value of $S_w^{\,*}$ near 0.13. Applying Eq. 6 using Eq. B2 for k_{rw} gives $S_w^{\,*}$ = 0.083, which is significantly less than the directly measured value

of 0.13. To accommodate this, we alter the exponent in Eq. B2 to 2.72, which gives $S_w^* = 0.13$. Thus in the end we use the following function for the model fit to the data of Ma et al.:

$$k_{rw} = 0.7888\left(\frac{S_w - S_{wc}}{1 - S_{wc} - S_{gr}}\right)^{2.7233} \quad \text{(B3)}$$

Of course in the absence of directly measured water saturations one would use the unadjusted $k_{rw}(S_w)$ function.

For fitting the foam data of Alvarez et al. (2001) in Berea sandstone we use relative-permeability functions based on data of Persoff et al. (1991) in Boise sandstone:

$$k_{rg} = 0.94\left(1 - \frac{S_w - S_{gr}}{1 - S_{wc} - S_{gr}}\right)^{1.3} \quad \text{(B4)}$$

$$k_{rw} = 0.20\left(\frac{S_w - S_{wc}}{1 - S_w - S_{wc}}\right)^{4.2} \quad \text{(B5)}$$

with $S_{wc} = S_{gr} = 0.2$.

For the foam experiments in Limestone of Chabert et al. (2012) we fit the relative-permeability data of Mohamed and Nasr-El-Din (2012) for low-permeability Indiana limestone with the following relations:

$$k_{rg} = 0.05\left(1 - \frac{S_w - S_{wc}}{1 - S_{wc} - S_{gr}}\right)^{1.02} \quad \text{(B6)}$$

$$k_{rw} = 0.28\left(\frac{S_w - S_{wc}}{1 - S_{wc} - S_{gr}}\right)^{2.41} \quad \text{(B7)}$$

with $S_{wc} = 0.32$ and $S_{gr} = 0.08$.